Chaotic Optical Communication Over 1000 km Transmission by Coherent Detection

Zhao Yang, Lilin Yi, *Member, IEEE*, Junxiang Ke, Qunbi Zhuge, *Member, IEEE*, Yunpeng Yang, and Weisheng Hu, *Member, IEEE*

***Abstract*—Chaotic optical communication was originally proposed to provide high-level physical layer encryption. For high-speed and long-distance transmission, chaotic signal is very sensitive to channel impairments such as dispersion and Kerr fiber nonlinearity. In the traditional chaotic optical communications, these impairments must be compensated in optical domain before chaos synchronization. However completely compensating the high-order dispersion and fiber nonlinearity in the optical domain has great challenges, therefore limiting the transmission distance of high-speed chaotic optical communications less than 150 km. Here we propose a method aiming to break the limit. Thanks to coherent detection, channel impairments can be compensated in the digital domain using various algorithms. Digital back propagation algorithm is used for jointly compensating linear and nonlinear impairments of the chaotic signals, constant modulus algorithm is used for channel equalization and extended Kalman filter is adopted for carrier phase recovery. After digital processing, the recovered chaos signal is converted back to the optical domain for chaos synchronization. By this means, we demonstrate a 10 Gb/s phase-modulation signal encrypted by phase chaos transmission over record-breaking 1000 km single-mode fiber with bit-rate error less than 1.0×10^{-3} by simulation, and support the results with extensive numerical analysis.**

***Index Terms*—Chaos, chaotic optical communications, coherent detection, digital signal processing.**

I. Introduction

CHAOS synchronization, proposed by Pecora and Carroll in 1990, has been used in optical communications to provide high-level physical layer encryption [1]. In past decades, many efforts have been dedicated to chaos synchronization and communications based on the nonlinearity of lasers and modulators due to their fast response and inherent compatibility with fiber optic networks [2], [3]. In 2005, Argyris *et al.* successfully demonstrated chaos-encrypted 1 Gb/s message transmission over 120 km fiber via a commercial fiber-optic network [4]. In 2010, Lavrov *et al.* reported that 10 Gb/s message, hidden in the phase of optical chaos, is transmitted over 120 km fiber in an installed fiber-optic network [5], [6]. And recently, Junxiang Ke *et al.* demonstrated a 30 Gb/s chaos-encrypted duobinary signal transmission over 100 km fiber [7]. Nevertheless, chaotic optical communications still encounter problems in high-speed and long-distance fiber transmissions. Chaotic carrier can be considered as analog signal and suffers from fiber channel impairments such as chromatic dispersion and nonlinearity [8]. In traditional chaotic receivers that employ direct detection, the phase of optical field is lost and receiver computes decision variables based on the measurement of signal energy. The loss of phase information is an irreversible transformation which prevents full equalization of channel impairments. Dispersion compensation fiber (DCF) or tunable dispersion compensator (TDC) must be used to compensate the second-order dispersion in optical domain, but higher-order dispersion and Kerr nonlinearity effects are difficult to be compensated [2], [3], [9]. These impairments have serious impact in long-haul transmission systems, limiting the transmission distance of high-speed chaotic optical communications. Until now, the transmission distance of chaotic optical communication beyond 10 Gb/s does not exceed 150 km.

Coherent detection circumvents this problem by combining the received chaotic signal with a local oscillator (LO) laser and by using balanced detection to down-convert it into a baseband electrical output that is proportional to the optical E-field [9]. The resulting chaotic signal can then be sampled and processed by digital signal processing (DSP) algorithms, providing a flexible platform based on a software that is an attractive alternative to optical channel impartments compensation [11]. In this paper, for the first time, we propose to use coherent detection to mitigate the transmission impairments of the chaotic signals in the digital domain rather than the optical domain after long-haul transmission. Coherent detection combined with DSP algorithms has great significant advantages in dealing with fiber impairments. DSP algorithms can completely compensate any-order dispersion and tremendously reduce the influence of nonlinearity [12]. Coherent detection has been widely used in digital optical communication systems. Here we prove it can also be used in chaotic optical communications to mitigate the impairments of analog chaotic signal with no optical dispersion compensation module. The chaotic signal is converted back to optical domain for chaos synchronization after digital signal processing. With coherent detection

Manuscript received December 8, 2019; revised February 24, 2020 and May 3, 2020; accepted May 5, 2020. Date of publication May 11, 2020; date of current version September 1, 2020. This work was supported by the National Key R&D Program of China under Grant 2018YFB1800904 *(Corresponding author: Lilin Yi.)*

The authors are with the State Key Lab of Advanced Optical Communication Systems and Networks, Shanghai Institute for Advanced Communication and Data Science, Shanghai Jiao Tong University, Shanghai 200240, China (e-mail: chongyang@sjtu.edu.cn; lilinyi@sjtu.edu.cn; junxiangke@sjtu.edu.cn; qunbi.zhuge@sjtu.edu; yyp9504@126.com; wshu@sjtu.edu.cn).

Color versions of one or more of the figures in this article are available online at https://ieeexplore.ieee.org.

Digital Object Identifier 10.1109/JLT.2020.2994155

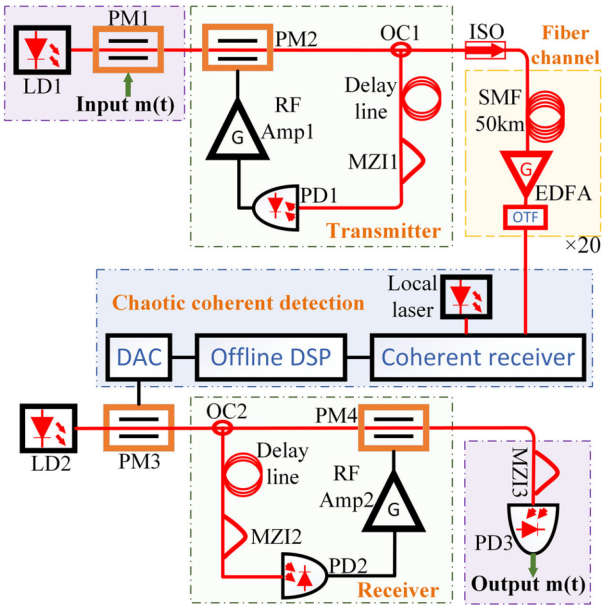

Fig. 1. Setup of the coherent phase chaos communication system. LD, laser diode; PM, phase modulator; OC, optical coupler; MZI, Mach–Zehnder interferometer; PD, photodiode; AMP, broadband radio frequency amplifier; ISO, optical isolator; SMF, single-mode fiber; EDFA, Erbium-doped fiber amplifier; OTF, optical tunable filter; DSP, digital signal processing; DAC, digital-to-analog converter. Fiber connections are represented by red lines and electrical connections by black lines.

and digital algorithms, we successfully demonstrate a 10 Gb/s differential-phase-shifted-keying (DPSK) signal encrypted by phase chaos transmission over 1000 km single mode fiber (SMF) with bit-error-rate (BER) less than 1.0×10^{-3} by simulation, and support the results with thorough analysis.

The structure of this paper is as follows. In Section II, the structure of the transmitter and receiver setup, along with the fiber transmission link and coherent receiver are presented. The channel impairments are briefly introduced and a comparative study of the direct detection and coherent detection has been carried out numerically in Section III. Blind algorithms for chaotic compensation are presented in Section IV. The chaotic synchronization performance and the BER performance of the decrypted DPSK signal are shown in Section V. Summary and conclusions are presented in Section VI.

II. Simulation Setup and Analysis

A. System Simulation Setup

The setup depicted in Fig. 1 shows the transmitter-receiver architecture of the coherent phase chaos communication system. A laser diode (LD1) followed by a phase modulator (PM1) performs the binary DPSK signal generation, which participates the oscillation of phase chaos. Inside the phase chaos generator, a delay line is used to tune the loop delay time and a Mach-Zehnder interferometer (MZI1) is used to realize the phase-to-intensity conversion. After optical-to-electrical conversion by photodiode (PD1), the signal is amplified by an electrical amplifier (AMP1) as the driven signal of PM2 to form the feedback loop. Thus, the optical phase of the light at the PM2 output is phase modulated according to its own delayed history. The chaos-masked signal is injected into the transmission line through an optical isolator (ISO). The transmission link includes 20 spans of 50 km SMF followed by an Erbium-doped fiber amplifier (EDFA) and a tunable optical filter (TOF) for out-of-band noise suppression. And there is no dispersion compensation module in transmission link. At the receiver side, coherent receiver followed by DSP module is used to mitigate the transmission impairments of the phase chaos-masked signal. A digital-to-analogue (DAC) is used to drive a new phase modulator (PM3) for generating the phase chaos-masked signal in the optical domain. The output of the PM3 is equivalent to the output of the phase chaos generator thanks to the coherent detection and the DSP module. Then the phase chaos can be cancelled in another phase generator whose parameters are matched with those in the chaotic transmitter. Finally, the decrypted DPSK signal is demodulated by a standard MZI3 to achieve the original binary message.

B. Mathematical Model oF Phase Chaos

A brief description of the phase chaos generation process at the transmitter is as follows: The dynamics follows nonlinear delay differential equations [4]. The nonlinear transformation is performed while modulating the phase condition in the MZI1, where the interferometer function and the phase modulation operation are split (see Fig. 1). The interferometer is imbalanced with a delay of δT, leading to an interference condition ruled by the phase difference between times t and $t-\delta T$. As soon as the phase modulation is performed faster (response time τ) than the time unbalancing ($\delta T >> \tau$), a dynamic scanning of the nonlinear interference modulation transfer function is achieved. In the phase chaos feedback loop, the nonlinearity is originated from the MZI and the nonlinearity function is as follows [6]:

$$f(t) \approx \beta cos^2[x(t-T) - x(t-T-\delta T) + \Phi_0] \quad (1)$$

Where $T = 2.5 \times 10^{-8}$ s stands for the total loop delay time, $\beta = 5$ is the normalized loop gain, $\Phi_0 = \pi/4$ is the offset interference phase and $\delta T = 4.0 \times 10^{-10}$ s is the imbalanced delay time of the interferometer. The differential nonlinear process ruling chaotic dynamics is derived from the bandpass filtering function of the optoelectronic feedback path including PM2, PD1 and AMP1. Such a filter can be approximated by two low and high cut-off frequencies, corresponding to an integral response time with $\theta = 5.0 \times 10^{-6}$ s, a differential response time with $\tau = 1.8 \times 10^{-11}$ s respectively. The corresponding high frequency is $\nu_{hf} = (2\pi \cdot \tau)^{-1}$ and the low frequency is $\nu_{lf} = (2\pi \cdot \theta)^{-1}$. These dynamics lead to the following phase chaos differential delay equation [6]:

$$\frac{1}{\theta}\int_{t_0}^{t} x(\zeta)d\zeta + x(t) + \tau\frac{dx(t)}{dt} = \beta cos^2[x(t-T) - x(t-T-\delta T) + \Phi_0] \quad (2)$$

The DPSK signal also participates the phase-chaos generation process to increase the chaos complexity. Then the phase chaos-masked signal is injected into the transmission link.

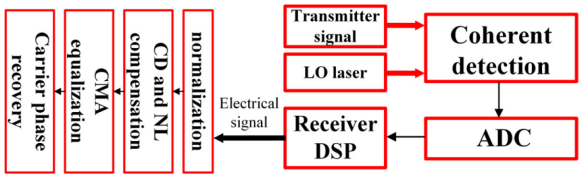

Fig. 2. Diagram of coherent receiver and following DSP algorithms.

C. Signal Propagation and Coherent Detection

Considering chromatic dispersion (CD) and self-phase modulation (SPM), the chaotic signal propagation in optical fiber channels could be described by a simplified version of nonlinear Schrodinger equation (NLSE) as [12]:

$$i\frac{\partial E(z,t)}{\partial z} = -\frac{i}{2}\alpha E + \frac{1}{2}\beta_2\frac{\partial^2 E}{\partial t^2} + \frac{i}{6}\beta_3\frac{\partial^3 E}{\partial t^3} - \gamma|E|^2 E \quad (3)$$

Where $E(z, t)$ is the slowly varying complex amplitude of optical field, and the fiber launch power is proportional to the square of $E(z, t)$. For SMF, $\alpha = 0.2$ dB/km is the attenuation coefficient, $\beta_2 = -20.39$ ps^2/km and $\beta_3 = 0.1$ ps^3/km are the typically second-order and third-order chromatic dispersion parameters, $\gamma = 1.31$ W^{-1}km^{-1} is the Kerr nonlinear coefficient, and z is the transmission distance. The span length is 50 km. EDFAs ideally compensate the transmission loss and introduce amplified spontaneous emission (ASE) noise with 5 dB noise figure. An OTF with a bandwidth of 0.1 nm is used to suppress the ASE noise in each span.

In the receiver side, coherent detection is used to achieve the amplitude and phase information of phase-chaos signal in the electric domain. The linewidth of both the transmitter laser and the local oscillator (LO) laser is set to 1 kHz, which is commercially available. Then DSP algorithms are used to compensate the impairments of the fiber channel. The adopted DSP algorithms must be format-independent because chaotic signal has the characters of non-periodic and random noise, so the receiver all uses blind algorithms to compensate the channel impairments. Fig. 2 shows the algorithm for each DSP block.

III. Fiber Channel and Receiver Structure

The chaotic signal during fiber propagation suffers lots of impairments such as chromatic dispersion, nonlinearity and so on. Direct detection and coherent detection have different methods and algorithms to compensate channel impairments. Here we first review the major channel impairments in fiber transmission and give a comparison between coherent detection and direct detection.

A. Channel Impairments

1) Chromatic Dispersion: Chromatic dispersion (CD) is caused by waveguide and material dispersion [14]. The effect of dispersion can be modeled as a linear filtering process. Chromatic dispersion can be described analytically as an all-pass filter in the frequency domain by [10]:

$$H_{CD}(\omega) = \exp\left[-j\left(\frac{1}{2}\beta_2 L(\omega-\omega_s)^2 + \frac{1}{2}\beta_3 L(\omega-\omega_s)^3\right)\right] \quad (4)$$

Where L is the length of the fiber, ω_s is the angle frequency of chaotic signal. For short-reach transmission, the second-order dispersion is dominant, and the third-order dispersion is almost negligible. But for long-distance chaotic transmission system, the influence of third-order dispersion cannot be ignored. The CD effect produces phase shift of the chaotic signal, thereby affecting phase synchronization [15]. If the phase shift increases beyond a certain limit, the synchronization of chaotic lasers may disappear, thereby resulting in a low correlation degree of chaotic synchronization.

2) Kerr Nonlinearity: The SPM effect gives rise to a phase-shift dependence of the optical intensity [12]. The nonlinearity experienced by a signal due to its own intensity and causes the spectrum broadening of the chaotic carrier. The fiber nonlinearity interacts with other channel impairments including chromatic dispersion and attenuation, and generate additional noise on the received symbols. Nonlinear noise compensation is the most difficult and challenging in the whole optical communication system and has serious impact in long-haul transmission system [16].

3) ASE Noise Caused by EDFAs: EDFAs are located at the end of each span to compensate for fiber attenuation and introduce amplified spontaneous emission (ASE) noise. An OTF with a bandwidth of 0.1nm (about 12.5 GHz at 1550 nm wavelength region) is used to suppress the ASE noise in each span. The gain in each span is $G = \exp(\alpha \cdot L_{span})$, where L_{span} is the span length of fiber channel. And the average power of ASE noise (N_{ASE}) [9]:

$$N_{ASE} = (NF \cdot G - 1) \cdot hf \cdot B_0 \quad (5)$$

Where NF is the noise figure of EDFA, h is Planck's constant, f is the optical chaotic frequency and B_0 is the bandwidth of OTF. ASE noise can be ignored in short distance transmission but in long-haul systems, interaction between ASE noise and chaotic signal through the Kerr nonlinearity leads to nonlinear phase noise (NLPN).

4) Laser Phase Noise: As mentioned above, coherent detection can get the phase information of chaotic signal. So, the influence of phase noise on chaotic synchronization degradation cannot be ignored. Laser phase noise caused by spontaneous emission of both transmitter and local laser is an important impairment in coherent systems, and is modeled as a Wiener process [17]:

$$\varphi(t) = \int_{-\infty}^{t} \delta\omega(\tau)d\tau \quad (6)$$

where $\varphi(t)$ is the instantaneous phase noise, the $\delta\omega(\tau)$ is mutually independence and identically distributed random Gaussian variables with zero mean and variance $\sigma_f^2 = 2\pi(\Delta\nu \cdot T_S)$, $\Delta\nu$ is the linewidth of chaotic transmitter and local lasers and T_S is the symbol period. The received baseband chaotic signal is modulated by $\exp(i\cdot\varphi(t))$. Chaotic synchronization is required

to ensure $\varphi(t)$ is small so the transmitted DPSK symbols can be detected with low power penalty.

B. Comparison Between Coherent Detection and Direct Detection at the Receiving End

Direct detection has the advantages of simple structure and low system complexity. In short distance transmission, the second-order dispersion is the main impairment. For dispersion compensation, optical compensation module like DCF or digital equalizer can be adopted. The optical dispersion compensation module can only compensate the second-order dispersion, which has great limitations on the compensation of the third-order dispersion and introduces nonlinearity. The loss of phase information prevents full equalization of dispersion compensation by digital equalizer. Meanwhile nonlinear compensation is a great challenge for direct detection. Although coherent detection increases the complexity of the system, compared with direct detection, it can effectively compensate the channel impairments through various algorithms at the receiver and greatly increase the transmission rate and distance. CD is a linear impairment in coherent detection system, which can be completely compensated by FIR filter algorithm without using optical dispersion compensation module [8]–[10]. For the third-order dispersion and nonlinearity which cannot be compensated by direct detection, coherent detection can accurately compensate any order dispersion and effectively compensate the nonlinearity by DSP algorithms. Especially for phase chaos, carrier phase recovery algorithms can be used for chaotic phase noise compensation. So, after contrast, coherent detection combined with DSP algorithms has more advantages than direct detection in fully and accurately compensating channel impairments for the chaotic optical communication system with long distance transmission.

IV. Digital Signal Processing Algorithms

A. Digital Backpropagation Algorithm for Jointly CD and NL Compensation

For the jointly CD and Kerr-nonlinearity compensation, digital backpropagation algorithm (DBP) is a universal and efficient technique [18]–[21]. Any order CD can be compensated and nonlinear noise can also be mitigated effectively. The total dispersion can be compensated in the digital domain, avoiding the extra cost and signal loss of the dispersion compensation module in the optical domain [22], [23]. The DBP is designed to solve an inverse NLSE based on split-step Fourier method (SSFM) to estimate the transmitted signal [24]. The fiber length is divided into a large number of small segments. In practice, fiber dispersion and nonlinearity are mutually interactive at any distance along the fiber. However, these mutual effects are small within one step and thus the effects of dispersion and nonlinearity are assumed to be statistically independent of each other. As a result, SSFM can separately define two operators: (1) the linear operator that involves attenuation and dispersion effects and (2) the nonlinearity operator that takes into account fiber nonlinearities. These linear and nonlinear operators are formulated as follows:

$$D = -\frac{i}{2}\beta_2\frac{\partial^2}{\partial t^2} + \frac{1}{6}\beta_3\frac{\partial^3}{\partial t^3} - \frac{\alpha}{2}N = i\gamma|E|^2 \tag{7}$$

And the inverse NLSE can be reweitten in a shorter form:

$$\frac{\partial E}{\partial(-z)} = (D+N)E \tag{8}$$

the complex amplitudes of optical pulses propagating from z to $z+\Delta z$ are calculated using the approximation shown here:

$$E(z+\Delta z, T) \approx \exp\left(\frac{\Delta z}{2}D\right)\exp\left(\int_z^{z+\Delta z} N(z')dz'\right)\exp\left(\frac{\Delta z}{2}D\right)E(z,T) \tag{9}$$

First, the optical pulse propagates through the linear operator that has a step size of in which the fiber attenuation and dispersion effects are taken into account. Then, the fiber nonlinearity is calculated in the middle of the segment. After that, the pulse propagates through the second half of the linear operator. The process continues repetitively in consecutive segments of size $\Delta z = 20$ m until the end of the fiber. It should be highlighted that the linear operator is computed in the frequency domain while the nonlinear operator is calculated in the time domain so fast Fourier transform (FFT) algorithm is used in each iteration.

B. Constant Modulus Algorithm for Channel Equalization

We know the amplitude of the phase chaos and DPSK signal is constant. So, after CD and nonlinearity compensation, constant modulus algorithm (CMA) is used for channel equalization. CMA is a blind algorithm which adapts the filter coefficients of the equalizer to reduce inter-symbol interference (ISI) of the received signal [25], [26]. The CMA algorithm minimizes the error power between the equalized chaotic output and constant amplitude of chaotic carrier. And the CMA algorithm only uses the amplitude information of the chaotic carrier and does not involve the phase information. Let W denote the impulse response of the equalizer, $x(k)$ is the input chaotic carrier, the output as $y(k) = \mathrm{W}^{\mathrm{T}}(k)x(k)$, where $\mathrm{W} = [\mathrm{w}_0(k), \mathrm{w}_1(k), \ldots, \mathrm{w}_{\mathrm{N}-1}(k)]$ is the equalizer tap weights vector and N is the length of the equalizer. The cost function of CMA is of the form [27]:

$$J(k) = E\left[\left(|y(k)|^2 - 1\right)^2\right] \tag{10}$$

Where $E[\cdot]$ indicates statistical expectation. Using a stochastic gradient of the cost function $J(k)$ with respect to the tap weights vector $\mathrm{W}(k)$, the tap weights vector of the equalizer is adapted by [27]:

$$W(k+1) = W(k) + \mu \cdot e(k) \cdot y(k) \cdot x^H(k) \tag{11}$$

Where μ is the step size and $e(k)$ is the error signal given by $e(k) = 1 - |y(k)|^2$ [14]. Compared with digital signals, the blind equalization of chaotic signals requires more tap coefficients $N = 51$ and a smaller step size $\mu = 5 \times 10^{-4}$ to ensure the convergence of chaotic sequences. Clearly, for the phase chaos and DPSK signals, this criterion is optimal in the sense that for

perfect equalization, the error $e(k) \approx 0$, as the chaotic carriers all lie on a ring in the constellation.

C. Extended Kalman Filter For Carrier Phase Recovery

Phase noise is a Wiener process with temporal correlation and can be mitigated by extended Kalman filter (EKF) [28]. The EKF addresses the problem of estimating the states of a nonlinear dynamical system from noisy measurements. The EKF is a blind scheme to recursively estimate the current state by considering the past estimates and the current observations [29]–[31]. It also provides an optimal estimate in the sense of the minimum mean squared error, even though the evolution process for the state fluctuates randomly and the observation process is disturbed by noise [32], [33]. The EKF can be used to estimate the state of a chaotic system and synchronize two chaotic systems [34]. As the EKF-based method recovers the transmitted signal without any knowledge about the transmitted signal, the equalizer is considered as a "blind" equalizer.

For the phase chaos differential delay system [32]:

$$\begin{aligned} \dot{x(t)} &= f(x(t), x(t-T), u(t)) \\ y(t) &= h(x(t)) + n(t) \end{aligned} \tag{12}$$

Where $x(t)$ is the chaotic state, $u(t)$ is the control input, $y(t)$ is the measured output, T donates the time delay and $n(t)$ is the phase noise. Symbol "·" represents the derivative operation. The receiver filter or observer is given by:

$$\begin{aligned} \dot{\hat{x}(t)} &= f(\hat{x}(t), \hat{x}(t-T), u(t)) + L(t)\left[y(t) - h(\hat{x}(t))\right] \\ \hat{y}(t) &= h(\hat{x}(t)) \end{aligned} \tag{13}$$

Where $\hat{x}(t)$ is the estimate state, and has the same dimension as state $x(t)$. $L(t)$ is the time varying observer gain:

$$L(t) = P(t)C^T(t)R^{-1} \tag{14}$$

R is a positive definite matrix and $P(t)$ is the solution of the modified Riccati differential equation [32]:

$$\begin{aligned} \dot{P(t)} = P(t)[A(t) - L(t)C(t)] + P(t)[A^T(t) - \delta I] \\ + Q + \kappa A_\tau(t) A_\tau^T(t) \end{aligned} \tag{15}$$

Here, $\delta > 0$ is a term that makes the system robust to the noise, $\kappa > 0$ is a delay term tuning scalar, I is the identity matrix. Q and R are positive definite matrices which are used as weighting matrices and with

$$\begin{aligned} A(t) &= \frac{\partial f(\hat{x}(t), \hat{x}(t-T), u(t))}{\partial x(t)} \\ A_\tau(t) &= \frac{\partial f(\hat{x}(t), \hat{x}(t-T), u(t))}{\partial x(t-T)} \\ C(t) &= \frac{\partial h(\hat{x}(t))}{\partial x(t)} \end{aligned} \tag{16}$$

By properly setting the parameters, the EKF-based filter is implemented in the full-state estimation of phase chaos. In our simulation, $\delta = 10$ and $\kappa = 14$. The initial condition of the Riccati differential equation was set as $P(0) = Q = I$ and $R = 0.02$. In such a way that estimate error is minimized by tuning the parameters.

D. Phase Chaos Synchronization

Phase chaos cancellation is achieved using the closed-loop receiver scheme [5]. The phase modulation in the receiver is ruled by a similar equation:

$$\begin{aligned} \frac{1}{\theta'} \int_{t_0}^{t} x'(\zeta) d\zeta + x'(t) + \tau' \frac{dx'(t)}{dt} \\ = -\beta' cos^2[x(t - T') - x(t - T' - \delta T') + \Phi'_0] \end{aligned} \tag{17}$$

where symbol "′" denotes the parameters or functions involved at the receiver, similar to the ones at the transmitter. When all receiver parameters are matched as closely as possible with the ones set at the emitter, the phase chaos cancelation is obtained.

The chaos synchronization is evaluated quantitatively, and the normalized cross-correlation function C is used to measure the chaos synchronization performance between emitter and receiver, which is defined as:

$$C = \frac{\langle [x(t) - \langle x(t) \rangle] [y(t) - \langle y(t) \rangle] \rangle}{\sqrt{\left\langle [x(t) - \langle x(t) \rangle]^2 \right\rangle \left\langle [y(t) - \langle y(t) \rangle]^2 \right\rangle}} \tag{18}$$

where $x(t)$ is the time trace of emitter, and $y(t)$ is the time trace of receiver, $\langle \cdot \rangle$ denotes average. The sampling rate of oscilloscope is set at $F_s = 100\,\mathrm{GSa/s}$, and 10 000 points are used to calculate cross correlation function.

V. Simulation Results

We use MATLAB to simulate the communication performances of the 1000 km chaotic optical transmission system. A Fourth-order Runge-Kutta algorithm is adopted to numerically represent Eq. (2) and Eq. (17) for the phase chaos generation and synchronization [35]. The simulation parameters of the coherent phase chaos system and fiber channel are shown in Table I:

A. Phase Chaos Synchronization After 1000 km Fiber Transmission

First, the performance of the phase chaos over 1000 km fiber transmission without encoded data has been studied. Fig. 3 shows the cross-correlation function C of phase chaos with different launch powers after the 1000 km fiber transmission. The blue line and the green line respectively represent the case where only the second-order dispersion is compensated and both the second-order dispersion and the third-order dispersion are compensated. When the launch power varies from -8 dBm to 8 dBm, C is all lower than 0.80. Therefore, for the 1000 km fiber transmission, compensating for only CD is insufficient. Especially the Kerr nonlinearity has great influence on the chaotic waveform at high launch power.

For joint CD and NL compensation, the DBP algorithm has good performance as the red line shows. When the launch power range is from -4 to 0 dBm, C can reach above 0.90 by using DBP algorithms. What's more, C can even reach to 0.96 when the launch power is from -4 to -2 dBm. DBP is very effective

TABLE I
SIMULATION PARAMETERS

Symbol	Quantity	Conversion from Gaussian and CGS EMU to SI [a]
λ	wavelength of chaos	1550 nm
T	total loop delay	2.5×10^{-8} s
δT	interferometer delay	4.0×10^{-10} s
β	normalized loop gain	5
Φ_0	offset phase	$\pi/4$
θ	integral response time	5.0×10^{-6} s
τ	differential response time	1.8×10^{-11} s
α	attenuation coefficient	0.2 dB/km
β_2	second-order dispersion	-20.39 ps^2/km
β_3	third-order dispersion	0.1 ps^3/km
γ	Kerr nonlinear coefficient	1.31 W^{-1} km^{-1}
NF	Noise figure of EDFA	5 dB
L_{span}	span length of fiber	50 km
B_0	bandwidth of OTF	12.5 GHz
Δz	step length of SSFM	20 m
F_s	sampling rate	100 GSa/s
N	tap coefficients of CMA	51
μ	step size of CMA	5×10^{-4}

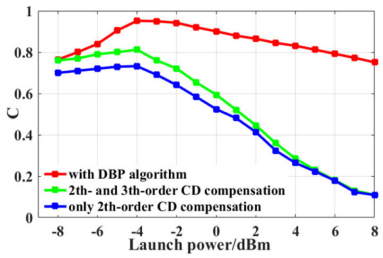

Fig. 3. Cross-correlation function C of phase chaos with different launch power using different algorithms.

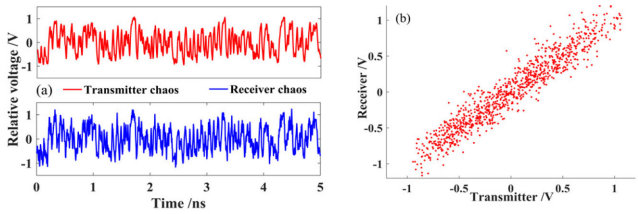

Fig. 4. (a) Time series of chaos by using DBP algorithm; (b) Chaotic synchronization plot of the emitter and receiver time series.

for nonlinearity compensation over a wide range of power variations, which can still achieve high cross correlation function C when the launch power is large. The chaotic waveforms before and after the 1000 km transmission are well matched by using the DBP algorithm. And the time series of chaos and chaotic synchronization plot of the emitter and receiver time series are shown in Fig. 4, demonstrating the powerful compensation capability of the DBP algorithm.

In the following simulation results, the DBP algorithm is used in receiver. The influence of the phase noise caused by the transmitter laser and local laser on the cross-correlation function is shown in Fig. 5. The red line represents using EKF for carrier phase recovery while the blue line represents that no carrier phase recovery algorithm is used. When the linewidth is 1 kHz, C can reach to 0.96. But when the linewidth is 100 kHz, C drops

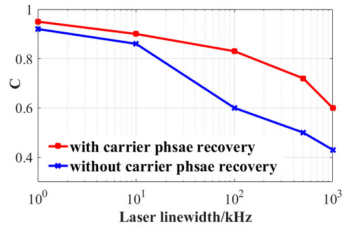

Fig. 5. Cross-correlation function C of phase chaos with different laser linewidths of transmitter laser and LO laser.

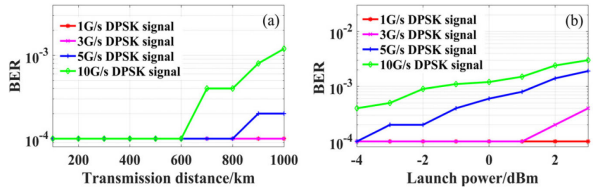

Fig. 6. BER performance of decrypted DPSK signals (a) BER performance with different transmission distances. (b) BER performance with different launch powers for 1000 km fiber transmission.

to 0.83. We can see that the chaotic signal is sensitive to phase noise, so it is necessary to use 1 kHz narrow linewidth lasers.

B. BER Performance of Decrypted DPSK Signal

Then we add the DPSK signal into the phase chaos generator and evaluate the system performance. As mentioned above, the step size of DBP algorithm is set to 20 m in order to obtain more accurate nonlinear compensation effect. We know that simulation of more bits will get a more accurate BER curve. But limited by the complexity of simulation system algorithms, Pseudo-random bit sequence (PRBS) with a sequence length of 10^4 is used to generate the DPSK signal. So, the lowest bit error rate is in the order of 10^{-4}, resulting in a BER floor of 1×10^{-4} in Fig. 6.

The launch power of the phase chaos-masked signal into the fiber is set at -2 dBm. The BER curves for the decrypted DPSK signal with different transmission distances are calculated and shown in Fig. 6(a). The red line and purple line are the BER performance of the 1 Gb/s and 3 Gb/s decrypted signals, where the number of bit errors is 0 after the 1000 km fiber transmission. For the blue line of the 5 Gb/s signal, when the transmission distance is less than 800 km, BER is nearly 0. And after 1000 km transmission the BER is below 4.0×10^{-4}. There is a similar trend for the 10 Gb/s signals with green line: when the transmission distance is less than 600 km, the BER can be reduced to 0 by compensating channel impairments. As the transmission distance increases, the BER begins to increase gradually. When the transmission is 1000 km, the bit error rate is approximately 1.0×10^{-3}, which is the threshold of forward error correction (FEC).

Also, we simulate the BER of the decrypted DPSK signal at different launch powers for 1000 km fiber transmission, and the results are shown in Fig. 6(b). BER is positively correlated with launch power, because the stronger the launch power is, the stronger the nonlinearity is. The red line and purple line are the

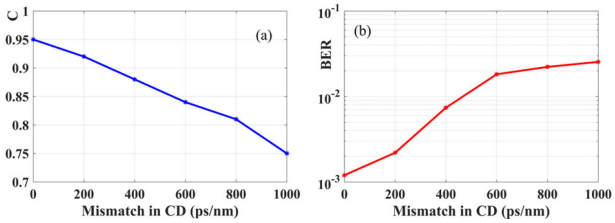

Fig. 7. (a) Cross correlation function C of phase chaos with mismatch in CD after 1000 km fiber transmission. (b) BER performance of decrypted 10 Gb/s DPSK signal with mismatch in CD after 1000 km fiber transmission.

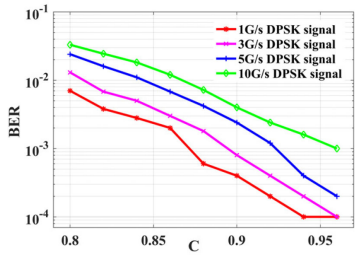

Fig. 8. BER performance of the decrypted DPSK signal with cross correlation functions C caused by parameters mismatch.

BER performance of the 1 Gb/s and 3 Gb/s decrypted signal, where the BER is nearly 0 after the 1000 km fiber transmission when the launch power is lower than 1 dBm. For the 5 Gb/s signal represented by the blue line, when the launch power is varied from -4 dBm to 3 dBm, the BER is changed from 0 to 1.2×10^{-3}. The 10 Gb/s signal with green line has the same tendency: as the launch power increases, the BER gradually increases from 4.0×10^{-4} to 2.6×10^{-3}. So, at different launch powers, the change range of BER is not obvious, which shows that the coherent detection algorithms have good tolerance to nonlinearity.

For coherent system, it would be useful to know how accurately CD has to be compensated to achieve acceptable performance. So, we simulate the cross-correlation function and BER of the decrypted 10 Gb/s DPSK signal with different mismatches in CD for 1000 km fiber transmission at -2 dBm launch power in Fig. 7. When the mismatch in CD increases from 0 to 1000 ps/nm, the BER increases from 1.2×10^{-3} to 2.54×10^{-2}. Strictly speaking, to ensure that C is larger than 0.9, it is better to control the mismatch of CD within 300 ps/nm.

C. Mismatched Parameters on Chaos Synchronization Quality

Usually, the feedback-loop chaotic parameters are difficult to be accurately controlled in practice, so it is necessary to investigate the influences of intrinsic mismatched parameters on chaos synchronization quality after 1000 km transmission. We keep the chaotic parameters of the transmitter unchanged, and a small random change is added to each parameter on the basis of ideal matching in receiver. The integral response time θ corresponds to tens of MHz, which barely has influence on chaos synchronization with the bandwidth of GHz magnitude. For the sake of convenience, we mainly study the effect of the mismatch of differential response time τ and normalized loop gain β on chaos synchronization. $\Delta\tau = \tau - \tau'$ and $\Delta\beta = \beta - \beta'$ are the mismatch between transmitter and receiver. And we can define the mismatch percent as $\Delta\tau / \tau = \Delta\beta / \beta$, the mismatch percent is changed from -0.2 to 0.2. The BER of the decrypted DPSK signal transmission over 1000 km fiber variation with the cross-correlation function caused by parameters mismatch is shown in Fig. 8. When C is less than 0.85, BER approaches to 1.0×10^{-2} for 10 Gb/s DPSK signal. Therefore, it is better to ensure that the parameters of the chaotic receiver and the transmitter are well matched and C is controlled above 0.9, which is achievable and in our previous experiment, $C = 0.95$ can be guaranteed [7].

VI. Conclusion

In conclusion, with coherent detection and DSP algorithms, a 10 Gb/s DPSK signal encrypted by phase chaos transmission over 1000 km SMF with BER less than 1.0×10^{-3} has been realized by simulation, aiming to solve the transmission limitations in the traditional direct detection-based chaotic optical communication systems. By using digital signal processing algorithms to compensate channel impairments including dispersion and nonlinearity, the chaotic synchronization coefficient after 1000 km fiber transmission can reach 0.96 with no optical dispersion compensation module. The simulation results prove the feasibility of long-haul transmission of chaotic optical communications and provide theoretical guidance for future experiments.

References

[1] L. M. Pecora and T. L. Carroll, "Synchronization in chaotic systems," *Phys. Rev. Lett.*, vol. 64, no. 8, pp. 821–824, Feb. 1990.
[2] D. Kanakidis, A. Bogris, A. Argyris and D. Syvridis, "Numerical investigation of fiber transmission of a chaotic encrypted message using dispersion compensation schemes," *J. Lightw. Technol.*, vol. 22, no. 10, pp. 2256–2263, Oct. 2004.
[3] J. G. Wu, Z. M. Wu and Y. R. Liu, Li Fan, Xi Tang, and G.-Q. Xia , "Simulation of bidirectional long-distance chaos communication performance in a novel fiber-optic chaos synchronization system," *J. Lightw. Technol.*, vol. 31, no. 3, pp. 461–467, Feb. 2013.
[4] A. Argyris *et al.*, "Chaos-based communications at high bit rates using commercial fibre-optic links," *Nature*, vol. 438, pp. 343–346, Nov. 2005.
[5] R. Lavrov, M. Peil, M. Jacquot, L. Larger, V. Udaltsov, and J. Dudley, "Electro-optic delay oscillator with nonlocal nonlinearity: Optical phase dynamics, chaos, and synchronization," *Phys. Rev. E.*, vol. 80, no. 2, Aug. 2009, Art. no. 026207.
[6] R. Lavrov, M. Jacquot, and L. Larger, "Nonlocal nonlinear electro-optic phase dynamics demonstrating 10 Gb/s chaos communications," *IEEE J. Quantum Electron*, vol. 46, no. 10, pp. 1430–1435, Oct. 2010.
[7] J. X. Ke *et al.*, "Chaotic optical communications over 100-km fiber transmission at 30-Gb/s bit rate," *Opt. Lett.*, vol. 43, no. 6, pp. 1323–1326, Mar. 2018.
[8] H. Hu *et al.*, "Electro-optic intensity chaotic system with varying parameters," *Phys. Lett. A*, vol. 378, no. 3, pp. 184–190, 2014.
[9] R. M. Nguimdo, R. Modeste, P. Colet, M. Jacquot, Y. K. Chembo, and L. Larger, "Effect of fiber dispersion on broadband chaos communications implemented by electro-optic nonlinear delay phase dynamics," *J. Lightw. Technol.*, vol. 28, no. 18, pp. 2688–2696, Sep. 2010.
[10] E. Ip, "Coherent detection in optical fiber systems," *Opt. Express*, vol. 16, no. 2, pp. 753–791, Jan. 2008.
[11] J. X. Ke, L. L. Yi and W. S. Hu, "Chaos synchronization error compensation by neural network," *IEEE Photon. Technol. Lett.*, vol, 31, no. 13, pp. 1104–1107, Jul. 2019.

[12] G. Bosco, "Advanced modulation techniques for flexible optical transceivers: The rate/reach tradeoff," *J. Lightw. Technol.*, vol. 37, no. 1, pp. 36–49, Jan. 2010.
[13] G. P. Agrawal, "Nonlinear fiber optics," in *Nonlinear Science At The Dawn oF The 21st Century*. Berlin, Germany: Springer, 2000, pp. 195–211.
[14] S. J. Savory, "Digital filters for coherent optical receivers," *Opt. Express*, vol. 16, no. 2, pp. 804–817, Nov. 2008.
[15] G. Kat, S. Dan, and T. Joseph, "Electrical dispersion compensation equalizers in optical direct-and coherent-detection systems," *IEEE Trans. Commun.*, vol. 54, no. 11, pp. 2045–2050, Nov. 2006.
[16] D. Rafique, "Fiber nonlinearity compensation: Commercial applications and complexity analysis," *J. Lightw. Technol.*, vol. 34, no. 2, pp. 544–553, Jan. 2016.
[17] M. G. Taylor, "Phase estimation methods for optical coherent detection using digital signal processing," *J. Lightw. Technol.*, vol. 27, no. 7, pp. 901–914, Apr. 2009.
[18] E. Ip and J. M. Kahn, "Compensation of dispersion and nonlinear impairments using digital backpropagation," *J. Lightw. Technol.*, vol. 26, no. 20, pp. 3416–3425, Oct. 2008.
[19] L. B. Du and A. J. Lowery, "Improved single channel backpropagation for intra-channel fiber nonlinearity compensation in long-haul optical communication systems," *Opt. Express*, vol. 18, no. 16, pp. 17075–17088, Aug. 2010.
[20] L. Galdino, "On the limits of digital back-propagation in the presence of transceiver noise," *Opt. Express*, vol. 25, no. 4, pp. 4564–4578, Feb. 2017.
[21] F. Zhang *et al.*, "Blind adaptive digital backpropagation for fiber nonlinearity compensation," *J. Lightw. Technol.*, vol. 36, no. 9, pp. 1746–1756, May. 2018.
[22] Q. Zhuge, M. Morsy-Osman, M. Chagnon, X. Xu, M. Qiu, and D. V. Plant, "Terabit bandwidth-adaptive transmission using low-complexity format-transparent digital signal processing," *Opt. Express*, vol. 22, pp. 2278–2288, Feb. 2014.
[23] Y. Gao, J. H. Ke, K. P. Zhong, J. C. Cartledge, and S. S. H. Yam, "Assessment of intrachannel nonlinear compensation for 112 Gb/s dual-polarization 16 QAM systems," *J. Lightw. Technol.*, vol. 30, no. 24, pp. 3902–3910, Dec. 2012.
[24] O. V. Sinkin, R. Holzlohner and J. Zweck, and C. R. Menyuk, "Optimization of the split-step Fourier method in modeling optical-fiber communications systems," *J. Lightw. Technol.*, vol. 21, no. 1, pp. 61–68, Jan. 2003.
[25] R. Johnson, P. Schniter and T. J. Endres, J. D. Behm, D. R. Brown, and R. A. Casas, "Blind equalization using the constant modulus criterion: A review," *Proc. IEEE*, vol. 86, no. 10, pp. 1927–1950, Oct. 1998.
[26] J. H. Zhou and Y. W. Zhang, "Blind time domain nonlinear compensator embedded in the constant modulus algorithm," *Opt. Express*, vol. 27, no. 16, pp. 22794–22807, Jul. 2019.
[27] K. Kikuchi, "Performance analyses of polarization demultiplexing based on constant-modulus algorithm in digital coherent optical receivers," *Opt. Exp.*, vol. 19, no. 10, pp. 9868–9880, May. 2011.
[28] L. Pakala and B. Schmauss, "Extended Kalman filtering for joint mitigation of phase and amplitude noise in coherent QAM systems," *Opt. Express*, vol. 24, no. 6, pp. 6391–6401, Mar. 2016.
[29] T. Raff and F. Allgöwer, "An EKF-based observer for nonlinear timedelay systems," in *Proc. Amer. Control Conf.*, Jun. 14–16, 2006, pp. 3130–3133.
[30] K. Fallahi, R. Raoufi, and H. Khoshbin, "An application of Chen system for secure chaotic communication based on extended Kalman filter and multi-shift cipher algorithm," *Commun. Nonlinear Sci. Numer. Simul.*, vol. 13, no. 4, pp. 763–781, Jul. 2008.
[31] H. Trinh and Q. P. Ha, "State and input simultaneous estimation for a class of time-delay systems with uncertainties," *IEEE Trans. Circuits Syst. II, Express Briefs*, vol. 54, no. 6, pp. 527–531, Jun. 2007.
[32] O. Hugues-Salas and K. A. Shore, "An extended Kalman filtering approach to nonlinear time-delay systems: Application to chaotic secure communications," *IEEE Trans Circuits Syst. I*, vol. 57, no. 9, pp. 2520–2530, Sep. 2010.
[33] Z. W. Zhu and H. Leung, "Adaptive blind equalization for chaotic communication systems using extended-Kalman filter," *IEEE Trans. Circuits Syst. I: Fundam. Theory Appl.*, vol. 48, no. 8, pp. 979–989, Aug. 2001.
[34] A. Kiani-B *et al.*, "A chaotic secure communication scheme using fractional chaotic systems based on an extended fractional Kalman filter," *Commun. Nonlinear Sci. Numer. Simul.*, vol. 14, no. 3, pp. 863–879, Mar. 2009.
[35] J. R. Dormand and P. J. Prince, "A family of embedded runge-kutta formulae," *J. Comput. Appl. Math.*, vol. 6, no. 1, pp. 19–26, Mar. 1980.